

# CLIP-GUIDED SOURCE-FREE OBJECT DETECTION IN AERIAL IMAGES

Nanqing Liu<sup>1,2</sup>, Xun Xu<sup>2</sup>, Yongyi Su<sup>2</sup>, Chengxin Liu<sup>2</sup>, Peiliang Gong<sup>2</sup>, Heng-Chao Li<sup>1</sup>

<sup>1</sup>School of Information Science and Technology, Southwest Jiaotong University, PR China

<sup>2</sup>Institute for Infocomm Research (I2R), A\*STAR, Singapore

## ABSTRACT

Domain adaptation is crucial in aerial imagery, as the visual representation of these images can significantly vary based on factors such as geographic location, time, and weather conditions. Additionally, high-resolution aerial images often require substantial storage space and may not be readily accessible to the public. To address these challenges, we propose a novel Source-Free Object Detection (SFOD) method. Specifically, our approach begins with a self-training framework, which significantly enhances the performance of baseline methods. To alleviate the noisy labels in self-training, we utilize Contrastive Language-Image Pre-training (CLIP) to guide the generation of pseudo-labels, termed CLIP-guided Aggregation (CGA). By leveraging CLIP’s zero-shot classification capability, we aggregate its scores with the original predicted bounding boxes, enabling us to obtain refined scores for the pseudo-labels. To validate the effectiveness of our method, we constructed two new datasets from different domains based on the DIOR dataset, named DIOR-C and DIOR-Cloudy. Experimental results demonstrate that our method outperforms other comparative algorithms. The code is available at <https://github.com/Lans1ng/SFOD-RS>.

**Index Terms**— Source-free domain adaptation, Object Detection, Aerial images, Self-training, CLIP.

## 1. INTRODUCTION

In recent years, object detection in aerial imagery [1, 2, 3, 4, 5] has seen growing interest due to its relevance in areas such as urban planning, environmental monitoring, and disaster management. Deep learning methods have been particularly successful in aerial object detection. However, these methods often exhibit limited generalization when applied to aerial images taken under various conditions, such as using different sensors or in different weather, leading to domain gaps or dataset biases.

To address these challenges, unsupervised domain adaptive object detection (UDAOD) has become a promising solution. Yet, UDAOD still depends on labeled data from the source domain, which poses a challenge in aerial imagery. High-resolution aerial images typically require substantial

storage space and may not be easily accessible to the public. To overcome these issues, source-free object detection (SFOD)[6] has been introduced. This approach relies solely on a pre-trained source model and an unlabeled target dataset. Most current SFOD researches [6] are based on self-training methods[7, 8], like the mean-teacher framework [9]. In this setup, a teacher model guides a student model, but there is a risk of error accumulation, known as *confirmation bias* if the teacher model provides incorrect learning targets.

Therefore, suppressing noisy labels generated during self-training is the key to solving this problem. Thanks to CLIP’s [10] outstanding abilities in zero-shot learning and domain adaptation, we utilize it to assist in generating pseudo-label scores across different domains. It is worth noting that in few-shot object detection, VFA[11] also employs CLIP as an auxiliary for scoring predicted boxes. However, unlike it, we employ CLIP on the teacher’s pseudo-labels to guide the student network’s learning, which is termed CLIP-guided Aggregation (CGA). Specifically, the labels generated by CLIP are compared with the pseudo-labels from the teacher model. If they match, the original classification scores are retained; if they differ, the pseudo-label scores are adjusted through weighted means. This approach leverages the CLIP model as an anchor in the learning process, helping to correct errors and reduce *confirmation bias*. To validate the effectiveness of our method, it needs to be tested on aerial images from different domains. The recent DOTA-C and DOTA-Cloudy datasets [12] introduced various corruptions to assess the robustness of detectors. However, this testing process can only be finished on DOTA servers and is relatively cumbersome. Therefore, based on this, we developed new datasets for different domains, namely DIOR-C and DIOR-Cloudy, derived from the DIOR dataset[3].

The main contributions of this paper are summarized as follows:

- To the best of our knowledge, we are the first to explore the SFOD method for oriented objects in aerial images.
- We integrate the CLIP into the teacher-student self-training pipeline, which somewhat alleviates the accumulation of errors in pseudo-labels.
- We develop two new datasets, DIOR-C and DIOR-

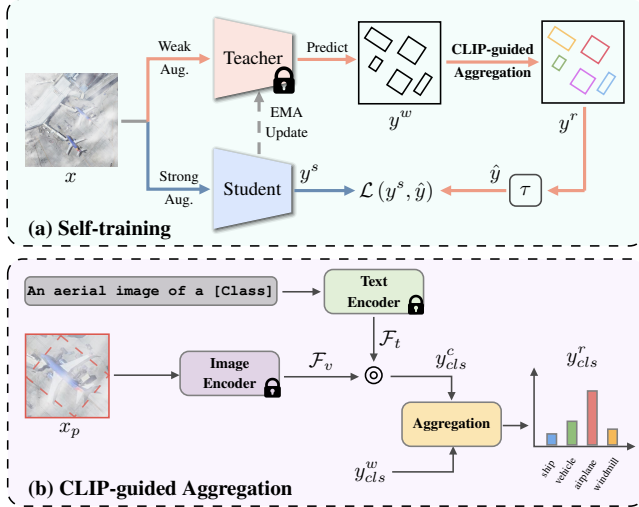


**Fig. 1.** Overall architecture of the proposed SFOD method. (a) Self-training framework. (b) CLIP-guided Aggregation.

Cloudy, for domain adaptation. Our method demonstrates improved performance on these datasets compared to other methods.

## 2. METHODOLOGY

In Source-Free Object Detection (SFOD), only the unlabeled target dataset  $\mathcal{D}_t$  and a pre-trained source model  $\Phi_p$  are utilized, without access to the labeled source dataset  $\mathcal{D}_s$ . As illustrated in Figure 1, we employ a self-training method specifically tailored for the target dataset [9]. In the pseudo-label generation phase, our method stabilizes pseudo-label scores by integrating CLIP-guided aggregation. This section will delve into these two key processes in detail.

### 2.1. Self-training

As illustrated in Fig.1(a), for a randomly selected target image  $x$  from the dataset  $\mathcal{D}_t$ , we employ both weak and strong augmentation methods to generate  $x^w$  and  $x^s$ , respectively. Weak augmentation is only horizontal flipping with a probability of 0.5. Strong augmentation includes a mix of color jittering, grayscale conversion, Gaussian blur, and Cutout. Both student and teacher models in our framework adopt the same network structure, specifically Oriented R-CNN [4].

For the weakly augmented images  $x^w$ , we input them into the teacher model  $\Phi_t$ . Post-processing techniques such as Non-Maximum Suppression (NMS) are then applied to derive the classification scores  $y_{cls}^w$  and regression parameters  $y_{reg}^w$  for oriented objects. Recognizing the potential imprecision in initial object box scores, we implement a CLIP-guided Aggregation operation to refine the class scores, resulting in adjusted scores  $y_{cls}^r$ . The detailed methodology of this operation will be discussed in the following section. A confidence threshold  $\tau$  is then used to filter out less probable predicted boxes, thus generating the final pseudo-labels  $\hat{y} = \{\hat{y}_{cls}, \hat{y}_{reg}\}$ .

In the parallel process for the strongly augmented images  $x^s$ , these are fed into the student model  $\Phi_s$ . This step similarly produces classification scores  $y_{cls}^s$  and regression parameters  $y_{reg}^s$  for oriented objects. The loss function is defined as:

$$\mathcal{L} = \mathcal{L}_{RoI} + \mathcal{L}_{RPN} \quad (1)$$

where  $\mathcal{L}_{RPN}$  and  $\mathcal{L}_{RoI}$  represent the losses for the Region Proposal Network (RPN) and the Region of Interest (RoI) head, respectively.

To reduce the negative impact of inaccurate pseudo-labels, we update the teacher model through an exponential moving average (EMA) scheme, defined as  $\Theta(\Phi_t) \leftarrow \alpha\Theta(\Phi_t) + (1 - \alpha)\Theta(\Phi_s)$ , with the coefficient  $\alpha$  set at 0.998.

### 2.2. CLIP-guided Aggregation

To prevent the self-training task from being biased by incorrect pseudo labels, we utilize the zero-shot capabilities of CLIP to help assess the predicted results by the teacher model. Since the predicted aerial targets are in rotated boxes, to input these patches into CLIP, we first need to transform these targets into horizontal style. Assuming the parameters of a rotated box are  $x, y, w, h, \theta$ , we calculate the width ( $w'$ ) and height ( $h'$ ) of the corresponding horizontal bounding box using the following equations:  $w' = w \cdot |\cos \theta| + h \cdot |\sin \theta|$ ,  $h' = w \cdot |\sin \theta| + h \cdot |\cos \theta|$ .

As shown in Fig.1(b), we then use this horizontal bounding box to extract the relevant patch from the original image, denoted as  $x_p \in \mathbb{R}^{N \times C \times H \times W}$ . Here,  $N$  represents the number of patches, while  $C$ ,  $H$ , and  $W$  denote the channels, height, and width, respectively. These patches  $x_p$  are fed into CLIP’s image encoder to obtain the feature embeddings  $\mathcal{F}_v \in \mathbb{R}^{N \times D}$ , where  $D$  is the dimensionality, typically 1024. Simultaneously, for the text branch, we formulate the text prompt simply as “An aerial image of a [Class]”, with [Class] being a placeholder for the various classes in the dataset. These prompts are processed by CLIP’s pre-trained text encoder, resulting in embeddings  $\mathcal{F}_t \in \mathbb{R}^{K \times D}$ , where  $K$  is the number of classes. The classification score  $y_{cls}^c \in \mathbb{R}^{N \times K}$  for each patch is then calculated as  $y_{cls}^c = \text{Softmax}(\|\mathcal{F}_v\| \cdot \|\mathcal{F}_t^T\|)$ .

Suppose the predicted classification score of the teacher model is  $y_{cls}^w \in \mathbb{R}^{N \times K}$ . Then we can employ the CGA to derive refined scores  $y_{cls}^r \in \mathbb{R}^{N \times K}$ , which is defined as follows:

$$y_{cls}^r = \begin{cases} y_{cls}^w, & \text{if } \text{argmax}(y_{cls}^w) = \text{argmax}(y_{cls}^c), \\ (1 - \lambda)y_{cls}^w + \lambda y_{cls}^c, & \text{otherwise.} \end{cases} \quad (2)$$

In this equation,  $\text{argmax}$  represents the category index with the highest value. The coefficient  $\lambda$  balances the original classification scores and those generated by CLIP. When the category predicted by CLIP matches the original score, indicating higher confidence in its accuracy, we keep the original score. Otherwise, we use a weighted combination of both scores

**Table 1.** Source-free domain adaptive object detection results on **DIOR-C** and **DIOR-Cloudy** dataset.

Model	DIOR-C																	DIOR-Cloudy		mAP		
	Ga.	Shot	Im.	Spec.	De.	Glass	Mo.	Zoom	Ga.	Snow	Frost	Fog	Br.	Spat.	Co.	El.	Pixel	JPEG	Sa.		Cloudy	
Clean	-	-	-	-	-	-	-	-	-	-	-	-	-	-	-	-	-	-	-	-	-	54.1
Direct test	13.1	12.2	13.6	15.6	28.5	24.4	29.4	18.6	29.6	22.8	25.8	36.3	<b>49.9</b>	34.0	32.7	43.7	40.1	47.5	<b>52.6</b>	39.0	30.5	
Tent[13]	15.8	14.6	16.4	16.6	19.5	16.4	21.9	11.9	20.6	16.3	18.2	26.8	28.5	21.6	27.5	26.1	26.5	25.8	30.4	23.6	21.3	
BN[14]	18.1	17.3	18.7	19.7	22.6	18.4	24.2	14.3	23.0	19.1	20.4	30.4	32.0	31.3	30.8	29.1	30.2	28.9	30.4	26.7	24.3	
Shot[15]	18.5	17.3	19.8	20.0	21.0	16.8	22.6	13.6	21.0	18.8	20.5	28.4	31.5	24.1	29.6	27.3	27.7	28.3	33.1	25.3	23.3	
Self-training[9]	24.1	<b>21.1</b>	24.2	25.0	36.4	35.4	39.7	27.8	39.1	30.0	31.9	47.7	47.9	38.8	47.5	45.6	45.9	46.7	50.1	42.1	37.4	
CGA (Ours)	<b>25.6</b>	20.1	<b>26.0</b>	<b>25.4</b>	<b>37.9</b>	<b>35.9</b>	<b>40.2</b>	<b>30.3</b>	<b>40.1</b>	<b>31.5</b>	<b>32.7</b>	<b>50.0</b>	49.3	<b>39.8</b>	<b>47.8</b>	<b>47.3</b>	<b>47.0</b>	<b>47.6</b>	51.9	<b>44.1</b>	38.5	

as the final score. This method effectively filters out unstable category scores and works independently of the teacher-student learning cycle, reducing the chance of spreading incorrect labels.

### 3. EXPERIMENTS

#### 3.1. Experimental Setup

The datasets currently available for evaluating different aerial image domains include DOTA-C [12] and DOTA-Cloudy [12]. However, these datasets have certain limitations. Specifically, evaluations on them require the use of DOTA’s server, and assessments for different types of corruption have to be conducted individually, posing significant challenges. To address this, we applied the corruptions from [12] to the DIOR dataset, resulting in two new datasets: DIOR-C and DIOR-Cloudy. DIOR-C incorporates 19 types of corruptions from ImageNet-C [16], categorized into four groups: **Noise** (Gaussian, Shot, Impulse, Speckle), **Blur** (Defocus, Glass, Motion, Zoom, Gaussian), **Weather** (Snow, Frost, Fog, Brightness, Spatter), and **Digital** (Contrast, Elastic transform, Pixelate, JPEG compression, Saturate). For our experiments, we only generated images with a severity level of 3. DIOR-Cloudy is synthesized using publicly available cloudy images from the DOTA-Cloudy dataset. We used the original DIOR training set as our source data and introduced the above corruptions to the original DIOR validation and test sets. For specific experimental details, readers can refer to the code we have released.

#### 3.2. Source-Free Object Detection Results

We adopt the following generic state-of-the-art source-free domain adaptation methods to object detection tasks. **Direct test**: Directly apply the source model to test on the target dataset. **BN** [14]: Updates batch normalization statistics on the target data during testing. **Tent** [13]: Adapt a model by the target data during testing. **Shot** [15]: Freeze the linear classification head and train the target-specific feature extraction module. **Self training** [9]: Two kinds of augmentation methods applying to target data. The pseudo-label is generated by the teacher network and used to supervise the student network.

We assess the performance of these methods on **DIOR-C** and **DIOR-Cloudy**, as detailed in Tab.1. The direct test-

ing results show a significant decrease compared to the clean test (from 54.1% to 30.5%), highlighting the substantial impact of image corruption. Notably, several source-free domain adaptive classification methods, such as Tent, BN, and Shot, demonstrate limited effectiveness when directly applied to detection tasks. The reason lies in classification methods often relying on statistics from large batch sizes for adaptation, which is not feasible in detection due to typically smaller batch sizes. Consequently, these methods sometimes perform even worse than direct testing. However, self-training significantly improved the results (from 30.5% to 37.4%), proving that it is very effective for SFOD in aerial images. Our method CGA, by incorporating CLIP, can further enhance the effectiveness of self-training. However, it is worth noting that our method does not show a significant improvement. This is because we only used the inference process of CLIP, and there is a gap between corrupted aerial images and CLIP. Therefore, its performance has not been fully exploited. In the future, we plan to decouple the text and image branches. This will allow us to adjust the scores for different texture categories accordingly.

We also visualize the results of different methods in Fig. 2. It can be observed that the direct test method exhibits instances of missed detections such as “*Vehicle*” and “*Ship*” due to domain shift. Although the self-training method can detect the required samples, it also introduces many false alarms, such as “*Baseball field*” and “*Expressway-Service-area*” due to the accumulation of errors during the training process. All methods overlooked the “*Harbor*” category in the detection results, but our method achieved the best performance.

#### 3.3. Ablation Study

We firstly assess the impact of varying  $\lambda$  values in Eq. 2. As depicted in Fig.3 (left), we observe that the optimal performance is achieved when  $\lambda$  is set to 0.2. Increasing  $\lambda$  further leads to a decline in effectiveness, indicating that excessive reliance on CLIP can negatively affect the network’s ability to generate accurate pseudo-labels. Additionally, we examine the influence of different CLIP encoder structures, as shown in Fig.3 (right). The results suggest that CNNs generally outperform transformers, mainly because the targets in aerial images are relatively simple. Consequently, transformers’ global information processing capabilities do not provide

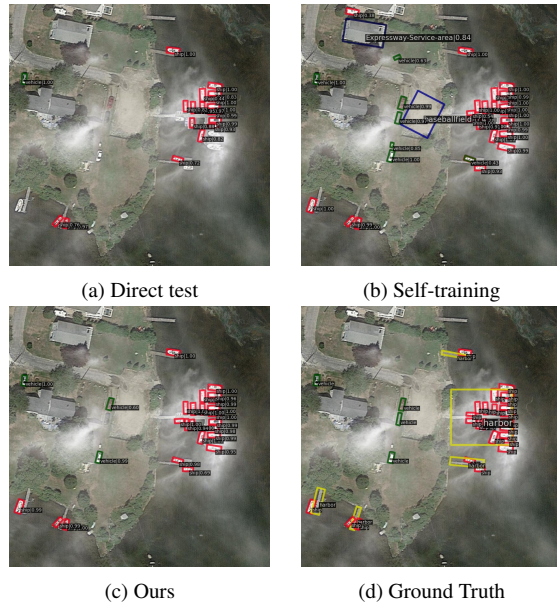


**Fig. 2.** Qualitative results of different methods on DIOR-Cloudy dataset.

substantial benefits in these scenarios.

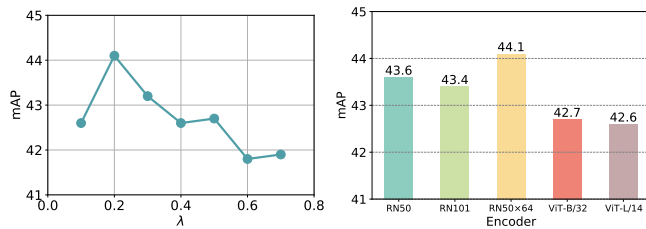


**Fig. 3.** Ablation experiments about different  $\lambda$  (left) and CLIP encoders (right) on the DIOR-Cloudy dataset.

## 4. CONCLUSION

The paper introduces a new method for source-free object detection in aerial images, which integrates CLIP to guide the generation of pseudo-label scores. Experiments were conducted on specially created datasets, DIOR-C and DIOR-Cloudy, derived from the publicly available DIOR dataset. The proposed method is simple yet effective, outperforming comparative SFOD methods. However, we observed that CLIP’s adaptability to certain types of corruption is limited. In the future, we plan to explore prompts designed specifically for different corruption to further improve performance.

## 5. REFERENCES

- [1] Nanqing Liu, Turgay Celik, Tingyu Zhao, Chao Zhang, and Heng-Chao Li, “Afdet: Toward more accurate and faster object detection in remote sensing images,” *IEEE J. Sel. Top. Appl. Earth Obs. Remote Sens.*, vol. 14, pp. 12557–12568, 2021.
- [2] Nanqing Liu, Xun Xu, Turgay Celik, Zongxin Gan, and Heng-Chao Li, “Transformation-invariant network for few-shot object detection in remote-sensing images,” *IEEE Trans. Geosci. Remote Sens.*, vol. 61, pp. 1–14, 2023.
- [3] Ke Li, Gang Wan, Gong Cheng, Liqiu Meng, and Junwei Han, “Object detection in optical remote sensing images: A survey and a new benchmark,” *ISPRS J. Photogramm. Remote Sens.*, vol. 159, pp. 296–307, 2020.
- [4] Xingxing Xie, Gong Cheng, Jiabao Wang, Xiwen Yao, and Junwei Han, “Oriented r-cnn for object detection,” in *Proc. IEEE Conf. Comput. Vis. Pattern Recognit.*, 2021, pp. 3520–3529.
- [5] Nanqing Liu, Xun Xu, Yingjie Gao, Yitao Zhao, and Heng-Chao Li, “Semi-supervised object detection with uncurated unlabeled data for remote sensing images,” *International Journal of Applied Earth Observation and Geoinformation*, vol. 129, pp. 103814, 2024.
- [6] Vibashan VS, Poojan Oza, and Vishal M Patel, “Instance relation graph guided source-free domain adaptive object detection,” in *Proc. IEEE Conf. Comput. Vis. Pattern Recognit.*, 2023, pp. 3520–3530.
- [7] Yongyi Su, Xun Xu, Tianrui Li, and Kui Jia, “Revisiting realistic test-time training: Sequential inference and adaptation by anchored clustering regularized self-training,” *arXiv preprint arXiv:2303.10856*, 2023.
- [8] Yongyi Su, Xun Xu, and Kui Jia, “Towards real-world test-time adaptation: Tri-net self-training with balanced normalization,” *Proc. AAAI Conf. Artif. Intell.*, 2024.
- [9] Yen-Cheng Liu, Chih-Yao Ma, Zijian He, Chia-Wen Kuo, Kan Chen, Peizhao Zhang, Bichen Wu, Zsolt Kira, and Peter Vajda, “Unbiased teacher for semi-supervised object detection,” *Proc. Int. Conf. Learn. Represent.*, 2021.
- [10] Alec Radford, Jong Wook Kim, Chris Hallacy, Aditya Ramesh, Gabriel Goh, Sandhini Agarwal, Girish Sastry, Amanda Askell, Pamela Mishkin, Jack Clark, et al., “Learning transferable visual models from natural language supervision,” in *Proc. Int. Conf. Mach. Learn.* PMLR, 2021, pp. 8748–8763.
- [11] Jiaming Han, Yuqiang Ren, Jian Ding, Ke Yan, and Gui-Song Xia, “Few-shot object detection via variational feature aggregation,” in *Proc. AAAI Conf. Artif. Intell.*, 2023.
- [12] Haodong He, Jian Ding, and Gui-Song Xia, “On the robustness of object detection models in aerial images,” 2023.
- [13] Dequan Wang, Evan Shelhamer, Shaoteng Liu, Bruno Olshausen, and Trevor Darrell, “Tent: Fully test-time adaptation by entropy minimization,” *Proc. Int. Conf. Learn. Represent.*, 2021.
- [14] Sergey Ioffe and Christian Szegedy, “Batch normalization: Accelerating deep network training by reducing internal covariate shift,” in *Proc. Int. Conf. Mach. Learn.* pmlr, 2015, pp. 448–456.
- [15] Jian Liang, Dapeng Hu, and Jiashi Feng, “Do we really need to access the source data? source hypothesis transfer for unsupervised domain adaptation,” in *Proc. Int. Conf. Mach. Learn.* PMLR, 2020, pp. 6028–6039.
- [16] Dan Hendrycks and Thomas Dietterich, “Benchmarking neural network robustness to common corruptions and perturbations,” *Proc. Int. Conf. Learn. Represent.*, 2019.